

# Forward delay in scaled $\text{Al}_{0.48}\text{In}_{0.52}\text{As}/\text{In}_{0.53}\text{Ga}_{0.47}\text{As}$ heterojunction bipolar transistors

J. A. Baquedano

*AT&T Microelectronica Espana, 28760 Tres Cantos, Madrid, Spain*

A. F. J. Levi

*Department of Electrical Engineering and Electrophysics, University of Southern California, Los Angeles, California 90089-1112*

B. Jalali

*Department of Electrical Engineering, University of California at Los Angeles, Los Angeles, California 90024*

A. Y. Cho

*AT&T Bell Laboratories, Murray Hill, New Jersey 07974*

(Received 24 May 1993; accepted for publication 5 August 1993)

We present experimental measurements and numerical simulations of the intrinsic forward delay as a function of base thickness in abrupt junction  $n$ - $p$ - $n$   $\text{Al}_{0.48}\text{In}_{0.52}\text{As}/\text{In}_{0.53}\text{Ga}_{0.47}\text{As}$  heterojunction bipolar transistors. For base thicknesses up to 1350 Å and impurity concentration  $p=1.5\times 10^{19}\text{ cm}^{-3}$  we find that nonequilibrium electron transport ensures that base transit delay is less than that in the 3000-Å-thick collector space-charge region. This provides an opportunity to increase base thickness and reduce base resistance without sacrificing the intrinsic forward delay time.

Figure 1 shows a schematic band diagram of an  $\text{Al}_{0.48}\text{In}_{0.52}\text{As}/\text{In}_{0.53}\text{Ga}_{0.47}\text{As}$   $n$ - $p$ - $n$  heterojunction bipolar transistor (HBT) under forward bias. The  $\Gamma$ -valley conduction-band minimum  $\text{CB}_{\text{min}}$ , the subsidiary conduction-band  $L$  minimum, and the valence-band maximum  $\text{VB}_{\text{max}}$ , are indicated. This structure is of particular interest because the large conduction band offset  $\Delta E_C=0.47\text{ eV}$  between the  $\text{Al}_{0.48}\text{In}_{0.52}\text{As}$  emitter and the  $\text{In}_{0.53}\text{Ga}_{0.47}\text{As}$  base results in extreme nonequilibrium electron transport in the base. It has previously been reported that this fact results in nonclassical scaling behavior in the static (dc) characteristics of the device. For example, breakdown voltage in the collector depends on base thickness  $x_B$  (Ref. 1) and current gain scales as  $1/x_B$  for devices with a thin base.<sup>2</sup> The physics governing these phenomena are intimately related to the temporal and spatial evolution of the nonequilibrium electron distribution initially injected into the base. In this letter, we report the effect such nonequilibrium electron dynamics has on the forward delay time of a transistor as a function of base thickness  $x_B$ .

The device structures are grown by solid-source molecular beam epitaxy on semi-insulating InP substrates using techniques described in Ref. 3. The  $\text{In}_{0.53}\text{Ga}_{0.47}\text{As}$  base of thickness  $x_B$  is Be doped to  $p=1.5\times 10^{19}\text{ cm}^{-3}$ . The  $\text{In}_{0.53}\text{Ga}_{0.47}\text{As}$  collector space-charge region is  $x_C=3000\text{ Å}$  thick and doped to  $n=1\times 10^{16}\text{ cm}^{-3}$ . Fabricated HBTs have an emitter stripe width of 2.5  $\mu\text{m}$ .

Figure 2(a) shows measured total forward delay time  $\tau_F=\tau_B+\tau_C$  as a function of base thickness  $200\text{ Å}<x_B<4000\text{ Å}$ .<sup>4</sup> Here,  $\tau_B$  and  $\tau_C$  are base and collector transit delays, respectively. The delay time is obtained by fitting the measured  $s$  parameters to the equivalent circuit model shown in the inset of Fig. 2(a). The error bars are a measure of fit sensitivity to a given set of equivalent circuit parameters. We note that, although the absolute value of

$\tau_F$  may slightly depend on the equivalent circuit model or the extraction method, in this letter we are only concerned with the relative change (i.e., the scaling behavior) of  $\tau_F$  for different  $x_B$ .

For base thickness less than approximately 1000 Å, the total forward delay is dominated by  $\tau_C$  and is therefore insensitive to variations in  $x_B$ . The measured delay time of  $\tau_F\approx\tau_C=0.5\pm 0.2\text{ ps}$  corresponds to an average electron velocity in the collector of approximately  $v_C\approx x_C/2\tau_C=3\times 10^7\text{ cm s}^{-1}$ . When  $x_B\gtrsim 1000\text{ Å}$  the base transit delay becomes important and  $\tau_F$  increases. For  $x_B=4000\text{ Å}$  we obtain  $\tau_F=6.7\text{ ps}$  and, since  $\tau_C$  remains essentially constant, we estimate  $\tau_B=6.2\text{ ps}$  corresponding to an average forward electron velocity in the base of  $v_B\approx x_B/\tau_B=6.4\times 10^6\text{ cm s}^{-1}$ . Obviously, the dramatic increase in base transit time delay can only be explained by a large change in average electron velocity with increasing base thickness  $x_B$ .

To understand the physics underlying these experimental results we performed numerical simulations similar to those described in Refs. 5–7. The electrons contributing to the emitter current,  $I_E$ , are initially thermally distributed in the conduction band of the wide band-gap  $\text{Al}_{0.48}\text{In}_{0.52}\text{As}$  emitter. Under forward base-emitter bias, electrons are injected with approximate excess kinetic energy  $\Delta E_C=0.47\text{ eV}$  into the  $\Gamma$ -valley conduction band of the  $p$ -type  $\text{In}_{0.53}\text{Ga}_{0.47}\text{As}$  base. There is also the possibility that some electrons enter the base, or subsequently scatter into the subsidiary  $L$  valley 0.55 eV above  $\text{CB}_{\text{min}}$  (see Fig. 1). The probability that electrons scatter elastically from statically screened ionized  $p$ -type impurities or inelastically off excitations of the degenerate  $p$ -type majority carriers while traversing the base may be calculated using the appropriate dielectric response function.<sup>8,9</sup> Electrons in the conduction band may also scatter off other conduction-

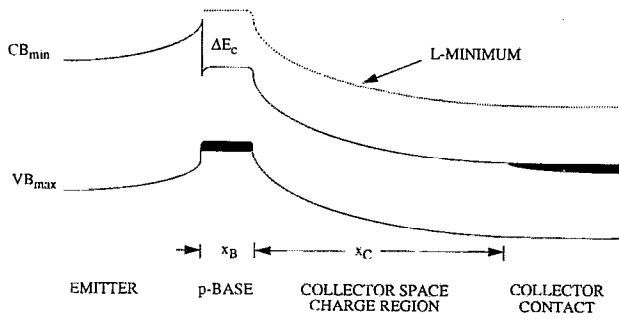


FIG. 1. Schematic band diagram of an  $n$ - $p$ - $n$   $\text{Al}_{0.48}\text{In}_{0.52}\text{As}/\text{In}_{0.53}\text{Ga}_{0.47}\text{As}$  HBT under forward bias.  $\Delta E_c = 0.47$  eV,  $p = 1.5 \times 10^{19}$   $\text{cm}^{-3}$ , and  $x_C = 3000$  Å.

band electrons. The model also takes into account the finite current gain of the transistor which arises from the fact that conduction-band electrons traversing the base can recombine with  $p$ -type majority carriers giving rise to base current  $I_B = (1 - \alpha) I_E$ . Having traversed the base, electrons are accelerated in the electric field of the reverse-

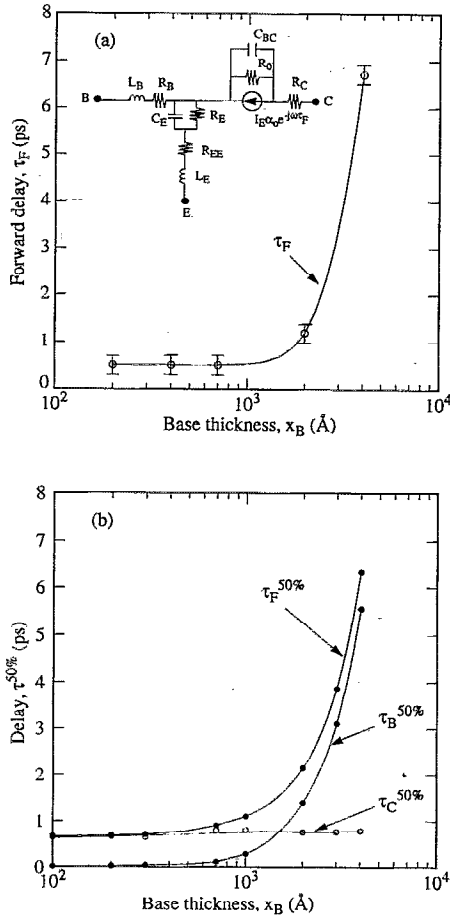


FIG. 2. (a) Small signal forward delay  $\tau_F$  for different base thicknesses  $x_B$ . The measurements were carried out at emitter current density of  $5 \times 10^4$   $\text{A cm}^{-2}$  and collector-emitter voltage bias  $V_{CE} = 1.5$  V. The error bars are  $\pm 0.2$  ps. The inset shows the equivalent circuit model used to model the device. (b) Results of calculating  $\tau_F^{50\%}$ ,  $\tau_B^{50\%}$ , and  $\tau_C^{50\%}$  as a function of base thickness for the device parameters used in the experiments.

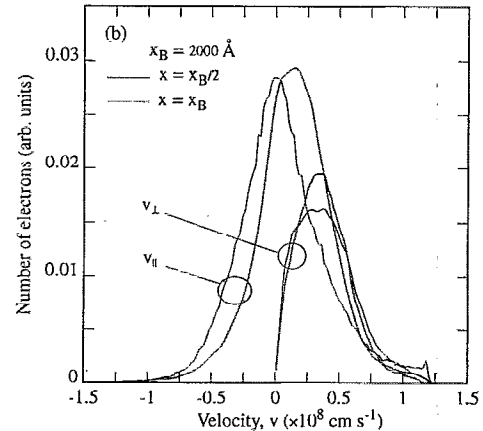
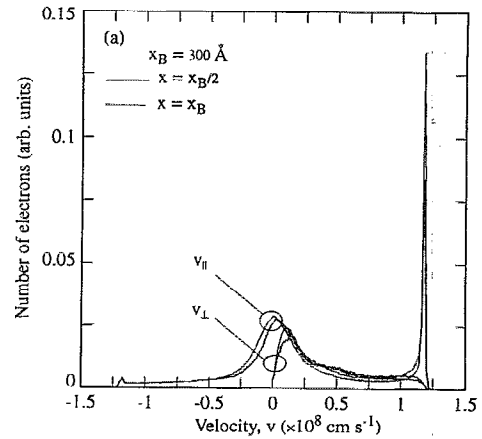


FIG. 3. Results of calculating the longitudinal (perpendicular to the plane of the heterojunction) electron velocity  $v_{||}$  and transverse electron velocity  $v_{\perp}$  distribution in the base of an  $\text{Al}_{0.48}\text{In}_{0.52}\text{As}/\text{In}_{0.53}\text{Ga}_{0.47}\text{As}$  HBT for  $x = x_B/2$  and  $x = x_B$  with (a)  $x_B = 300$  Å and (b)  $x_B = 2000$  Å.

biased collector space-charge region. Here they may suffer inelastic collisions with phonons and other electrons. Those electrons which gain enough kinetic energy may also transfer from the nonparabolic  $\Gamma$  valley to the high effective electron mass  $L$ - and  $X$ -valley conduction-band minima. In our model, trajectories of electrons are determined using a semiclassical Monte Carlo algorithm in which Poisson's equation is satisfied throughout the simulation.

In Fig. 2(b) we plot results of calculating the forward delay for 50% of step-injected current  $\alpha I_E$  to flow through the device  $\tau_F^{50\%}$ . Also shown are the contributions of  $\tau_B^{50\%}$  and  $\tau_C^{50\%}$  as a functions of base thickness  $x_B$ .  $\tau_B^{50\%}$  is the time for 50% of current  $\alpha I_E$  to flow across the base and  $\tau_C^{50\%}$  is the 50% large-signal delay across the collector. The results of our model are in good qualitative agreement with the experimental data shown in Fig. 2(a) even though the measured small-signal delay  $\tau_F$  is not identical to the calculated large-signal  $\tau_F^{50\%}$ . The numerical simulations clearly show that, although base transit delay increases with increasing  $x_B$ ,  $\tau_B$  does not become greater than  $\tau_C$  until  $x_B \geq 1350$  Å. In contrast, for a similar transistor but with diffusive base transport and diffusion constant  $D = 25$   $\text{cm}^2 \text{V}^{-1} \text{s}^{-1}$ ,  $\tau_B$  becomes greater than  $\tau_C$  when  $x_B \geq 600$  Å. Hence, the abrupt emitter/base junction HBT can have more than double the base thickness of the corresponding

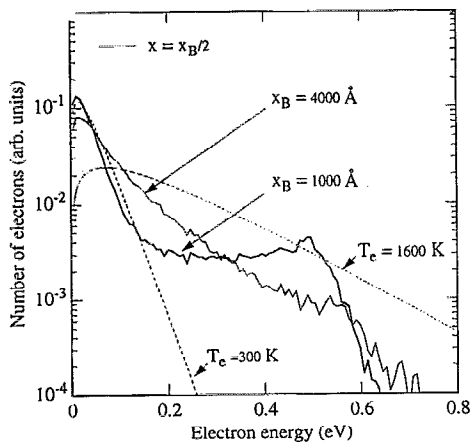


FIG. 4. Calculated electron energy distribution function at  $x_B/2$  for  $x_B = 1000 \text{ \AA}$  and  $x_B = 4000 \text{ \AA}$ . Dotted curves are the thermal electron distribution corresponding to an effective electron temperature  $T_e$ .

graded junction HBT without suffering a penalty in  $\tau_F$ .

To establish the role played by nonequilibrium electron transport in determining the trends in Figs. 2(a) and 2(b), in Fig. 3 we plot longitudinal and transverse electron velocity distribution in the base at  $x = x_B/2$  and  $x = x_B$  for (a)  $x_B = 300 \text{ \AA}$  and (b)  $x_B = 2000 \text{ \AA}$ . On the one hand, for a base thickness of  $x_B = 300 \text{ \AA}$  the peak in longitudinal electron velocity at approximately  $1.2 \times 10^8 \text{ cm s}^{-1}$  is due to extreme nonequilibrium electron transport across the base. On the other hand, the absence of any significant high velocity peak for  $x_B = 2000 \text{ \AA}$  is a clear indication that electrons have suffered many elastic and inelastic collisions. Nevertheless, even for  $x_B = 4000 \text{ \AA}$  the electron distribution function has not thermalized to the lattice temperature  $T = 300 \text{ K}$ . Of course, if the electron distribution could be described by some effective electron temperature  $T_e$ , we might consider introducing an effective diffusion constant  $D(T_e)$  to describe electron motion. However, as illustrated in Fig. 4, such an approach fails because, even for  $x_B \approx 4000 \text{ \AA}$ , the nonequilibrium electron distribution function *cannot* be described by an effective electron temperature  $T_e$ .

Although high-energy injection in abrupt junction

$\text{Al}_{0.48}\text{In}_{0.52}\text{As}/\text{In}_{0.53}\text{Ga}_{0.47}\text{As}$  HBTs results in nonequilibrium electron transport which does, in fact, reduce base transit delay, it may not be the optimum design in a transistor if device speed is limited by resistive and capacitive parasitics. In such a case it is necessary to carefully evaluate the relative advantages and disadvantages of abrupt versus graded emitter heterostructures.<sup>10</sup> In a graded device the turn-on voltage is reduced by approximately  $\Delta E_C$  resulting in reduced power dissipation. Furthermore, the collector current ideality factor  $n$  will be close to unity (compared to around  $n = 1.5$  for an abrupt junction  $\text{Al}_{0.48}\text{In}_{0.52}\text{As}/\text{In}_{0.53}\text{Ga}_{0.47}\text{As}$  HBT) resulting in a 33% reduction in emitter dynamic resistance  $r_E = nk_B T/qI_E$ , where  $k_B T$  is the thermal energy, and  $q$  is the electron charge. Therefore, if the base delay for diffusive transport can be tolerated, as usually occurs in a device dominated by parasitics, it may be beneficial to grade the emitter/base junction. On the other hand, it is important to note that the use of an abrupt emitter/base junction in the transistor of Fig. 1 allows for more than a factor of 2 thicker base for a given transit delay and this, of course, results in a lower base resistance. Reduction of base resistance is particularly important in devices with relatively large emitter dimensions. Thus, nonequilibrium electron transport provides an opportunity to reduce base resistance without suffering a penalty in base transit time.

<sup>1</sup>B. Jalali, Y. K. Chen, R. N. Nottenburg, D. Sivco, D. A. Humphrey, and A. Y. Cho, IEEE Electron. Device Lett. EDL-11, 400 (1990).

<sup>2</sup>A. F. J. Levi, B. Jalali, R. N. Nottenburg, and A. Y. Cho, Appl. Phys. Lett. 60, 460 (1992).

<sup>3</sup>A. Y. Cho, Thin Solid Films 100, 291 (1983).

<sup>4</sup>B. Jalali, A. F. J. Levi, S. L. Chuang, P. R. Smith, D. A. Humphrey, R. N. Nottenburg, D. Sivco, and A. Y. Cho, Proc. 4th International Conference on Indium Phosphide and Related Materials, Newport, RI, April 21-24 (IEEE, New York, 1992), p. 418.

<sup>5</sup>P. H. Beton and A. F. J. Levi, Appl. Phys. Lett. 55, 250 (1989).

<sup>6</sup>For a review of the Monte Carlo technique see, for example, C. Jacoboni and L. Reggiani, Rev. Mod. Phys. 55, 645 (1983); M. V. Fischetti and S. E. Laux, Phys. Rev. B 38, 9721 (1988); W. Faucett, A. D. Boardman, and A. D. Swain, J. Phys. Chem. Solids 31, 1963 (1970).

<sup>7</sup>Materials parameters taken from L. W. Massengill, T. H. Glisson, J. R. Hauser, and M. A. Littlejohn, Solid-State Electron. 29, 725 (1986).

<sup>8</sup>W. Bardyszewski and D. Yerick, Appl. Phys. Lett. 54, 837 (1989).

<sup>9</sup>A. F. J. Levi, Electron. Lett. 24, 1273 (1988).

<sup>10</sup>J. A. Baquedano, A. F. J. Levi, and B. Jalali (unpublished).